Model-Based Feedforward-Feedback Actuator Control for Real-Time Hybrid Simulation

Brian M. Phillips, A.M.ASCE[1]; and Billie F. Spencer Jr., F.ASCE[2]

Abstract: Substructure hybrid simulation is a powerful, cost-effective alternative for testing structural systems, closely coupling numerical simulation and experimental testing to obtain the complete response of a structure. In this approach, well-understood components of the structure are modeled numerically, while the components of interest are tested physically. Generally, an arbitrary amount of time may be used to calculate and apply displacements at each step of the hybrid simulation. However, when the rate-dependent behavior of the physical specimen is important, real-time hybrid simulation (RTHS) must be used. Computation, communication, and servohydraulic actuator limitations cause delays and lags that lead to inaccuracies and potential instabilities in RTHS. This paper proposes a new model-based servohydraulic tracking control method including feedforward-feedback links to achieve accurate tracking of a desired displacement in real time. The efficacy of the proposed approach is demonstrated through RTHS for a single-degree-of-freedom system and a 9-story steel building, each using a 200-kN large-scale magnetorheological damper as the rate-dependent physical specimen. **DOI: 10.1061/(ASCE)ST.1943-541X.0000606.**

CE Database subject headings: Hybrid methods; Simulation; Structural dynamics; Damping.

Author keywords: Real-time hybrid simulation; Actuator control; Actuator modeling; Structural dynamics; MR dampers.

Introduction

Earthquakes, strong winds, and tsunamis are among the most destructive forces that civil infrastructure faces. Advances in supplemental energy dissipation devices, such as base isolation, fluid dampers, and friction devices, provide promising solutions for mitigating damage from these dynamic loads (Soong and Spencer 2002). The responses of these devices are rate dependent, requiring real-time experimental evaluation. When these devices are used as part of a hybrid simulation, real-time execution of the experiment is necessary to obtain accurate and stable results [i.e., real-time hybrid simulation (RTHS)].

RTHS requires accurate tracking of a desired signal using servohydraulic actuators. Close examination of the system response shows that experimental equipment introduces both a time delay and frequency-dependent time lag into the RTHS loop. Time delays are not a function of frequency, generally being caused by the communication of data, analog-to-digital and digital-to-analog conversion, and computation time. These delays can be reduced by using faster hardware, smaller numerical integration time steps, and more efficient software. In contrast, time lags are a result of the physical dynamics and limitations of the servohydraulic actuators and vary with both the frequency of excitation and the specimen conditions (Dyke et al. 1995). Time delays and lags are an intrinsic part of experimental testing and mitigation of their effects is an essential part of RTHS.

A single apparent time delay, lumping together all of the actual time delays and time lags, was the basis for early efforts at real-time servohydraulic control for RTHS. For this reason, early approaches are referred to simply as delay compensation. One of the most widely used approaches for delay compensation is the polynomial extrapolation method (Horiuchi et al. 1996).

More recently, researchers have begun to address the servohydraulic system as a dynamic system, creating low-order transfer functions to represent the dynamics (Wallace et al. 2007; Chen and Ricles 2010). Inverses of these transfer functions can provide accurate compensation over the frequency range for which the transfer functions are accurate. When multiple-degree-of-freedom (MDOF) structures are lightly damped in higher modes, there is a potential for instabilities to manifest as a result of unmodeled high-frequency servohydraulic dynamics. A similar approach using a lead compensator to reduce phase lag was examined by Jung et al. (2007). These approaches are generally heuristic, designed to compensate for an observed time delay or time lag in the system.

Model-based servohydraulic control accounts directly for the frequency-dependent dynamics (both amplitude and phase) of the servohydraulic system over a broad frequency range through accurate modeling. Carrion and Spencer (2007) and Carrion et al. (2009) formulated the real-time servohydraulic control problem as a feedforward-feedback tracking problem, creating a model-based feedforward controller and introducing simplified feedback control. The feedforward controller was implemented as a model inverse with a low-pass filter to create a proper inverse. This research also included a scheduling control method whereby a feedforward controller was developed for each of the two extremes of the expected specimen conditions. A bumpless transfer was used to create a smooth transition between the feedforward controllers. The scheduling control method has merits for a specimen with behavior that is controlled by the user [e.g., the input current to magnetorheological (MR) dampers]; however, it is not generally applicable (e.g.,

[1]Doctoral Candidate, Dept. of Civil and Environmental Engineering, Univ. of Illinois at Urbana-Champaign, Urbana, IL 61801.

[2]Nathan M. and Anne M. Newmark Endowed Chair of Civil Engineering, Dept. of Civil and Environmental Engineering, Univ. of Illinois at Urbana-Champaign, Urbana, IL 61801 (corresponding author). E-mail: bfs@illinois.edu

Note. This manuscript was submitted on October 21, 2011; approved on March 2, 2012; published online on March 6, 2012. Discussion period open until December 1, 2013; separate discussions must be submitted for individual papers. This paper is part of the ***Journal of Structural Engineering***, Vol. 139, No. 7, July 1, 2013. ©ASCE, ISSN 0733-9445/2013/7-1205–1214/$25.00.

degrading structures). Also, the feedback controller uses a simple proportional gain but does not take advantage of the known dynamics of the system.

This paper proposes a systematic framework for model-based servohydraulic tracking control. The actuator tracking problem is reformulated as a regulator problem, and linear quadratic Gaussian (LQG) control theory is applied. A new approach to develop and implement the feedforward controller is presented that achieves excellent compensation over a broad frequency range. Additionally, a model-based feedback controller is designed to further improve tracking robustness and alleviate the need for online modification of the feedforward controller under changing specimen conditions. The efficacy of the model-based servohydraulic tracking control method proposed herein is demonstrated through RTHS of both a single-degree-of-freedom (SDOF) system and a 9-story steel building, each using a 200-kN large-scale MR damper as the physical specimen.

Problem Formulation

Substructure hybrid simulation provides an efficient and cost-effective means by which to test large, complex structures. By using substructing, this testing method saves the cost of constructing structural components in which the response is well understood and it greatly reduces the required laboratory space and equipment.

The equations of motion governing the structural response are solved using numerical integration with inputs from the numerically imposed force $\mathbf{F}^{\mathrm{N}}$ (e.g., caused by an earthquake) and measured restoring force $\mathbf{R}^{\mathrm{E}}$ from the experimental substructure. In discrete time form, the equations of motion can be written as

$$\mathbf{M}^{\mathrm{N}}\ddot{\mathbf{x}}_i + \mathbf{C}^{\mathrm{N}}\dot{\mathbf{x}}_i + \mathbf{R}_i^{\mathrm{N}} + \mathbf{R}_i^{\mathrm{E}}\left(\mathbf{x}^{\mathrm{E}}, \dot{\mathbf{x}}^{\mathrm{E}}, \ddot{\mathbf{x}}^{\mathrm{E}}\right) = \mathbf{F}_i^{\mathrm{N}} \tag{1}$$

where $\mathbf{M}^{\mathrm{N}}$ = mass matrix of the numerical substructure; $\mathbf{C}^{\mathrm{N}}$ = linear damping matrix of the numerical substructure; $\mathbf{R}_i^{\mathrm{N}}$ = restoring force vector of the numerical substructure; $\mathbf{R}_i^{\mathrm{E}}$ = restoring force vector of the experimental substructure; $\mathbf{F}_i^{\mathrm{N}}$ = vector of excitation forces; and $\mathbf{x}_i$, $\dot{\mathbf{x}}_i$, and $\ddot{\mathbf{x}}_i$ = vectors of displacement, velocity, and acceleration at time t_i (i.e., the ith time step), respectively. Here, $\mathbf{R}_i^{\mathrm{E}}$ is dependent on the displacement, velocity, and acceleration of the experimental substructure, or $\mathbf{x}^{\mathrm{E}}$, $\dot{\mathbf{x}}^{\mathrm{E}}$, and $\ddot{\mathbf{x}}^{\mathrm{E}}$, respectively.

The central difference method is one of the most common numerical integration schemes for RTHS (Nakashima et al. 1992; Darby et al. 1999; Horiuchi et al. 1999; Nakashima and Masaoka 1999; Horiuchi and Konno 2001; Wu et al. 2005; Carrion and Spencer 2007). The central difference method is based on the following relationships between displacement, velocity, and acceleration:

$$\dot{\mathbf{x}}_i = \frac{\mathbf{x}_{i+1} - \mathbf{x}_{i-1}}{2\Delta t} \tag{2}$$

$$\ddot{\mathbf{x}}_i = \frac{\mathbf{x}_{i+1} - 2\mathbf{x}_i + \mathbf{x}_{i-1}}{\Delta t^2} \tag{3}$$

where Δt = numerical integration time step. Eqs. (2) and (3) can be substituted into Eq. (1) to create an explicit representation of the displacement for advancing the numerical integration (i.e., the future displacements are only based on current and previous displacements). The central difference method is chosen in this study for its simplicity, although the proposed actuator control strategy can be used readily with other numerical integration schemes.

Throughout a hybrid simulation, communication between the experimental and numerical substructures is maintained in a loop of action and reaction as presented in Fig. 1. From numerical integration, the displacements $\mathbf{x}$ for the experimental substructure are calculated and sent to the loading system. The loading system, typically comprised of servohydraulic actuators, generates the physical displacements $\mathbf{x}^{\mathrm{E}}$ for the experimental substructure. The physical restoring force of the specimen $\mathbf{R}^{\mathrm{E}}$ is measured using sensors and returned to the numerical substructure as $\mathbf{R}^{\mathrm{E,meas}}$ for the next step of numerical integration.

In an ideal situation, the numerical substructure is directly coupled with the experimental substructure, meaning that $\mathbf{x}^{\mathrm{E}} = \mathbf{x}$ (perfect displacement tracking) and $\mathbf{R}^{\mathrm{E,meas}} = \mathbf{R}^{\mathrm{E}}$ (no delay/lag in the measurement of force). However, the loading system and sensors have their own inherent dynamics that are directly added into the dynamics of the closed-loop hybrid simulation. Rather than address the issue of time delay and time lag in a heuristic manner, control theory approaches will be used to develop accurate tracking control to directly address the sources of added (and unwanted) dynamics. In RTHS, sensors typically do not use filters such that they do not introduce lag, thus focus will be placed on the loading system.

Consider the input-output transfer function model $G_{yu}(s)$ of the linearized servohydraulic system, including the actuator, servovalve, servocontroller, and specimen, as represented in Fig. 2. The servocontroller contains inner-loop control (a proportional gain) to stabilize the servohydraulic system. In this model, e_{in} is the error between commanded and measured displacements, i_{c} is the command signal to the servovalve, Q_{L} is the oil flow through the load, p_{L} is the pressure drop across the load, and f_{P} is the force generated by the actuator piston. The proposed model-based servohydraulic tracking control approach uses feedforward and feedback control as an outer-loop controller around the servohydraulic system, such that the measured displacement y accurately tracks a desired displacement r (i.e., minimizing time delay, time lag, and amplitude errors).

The linearized dynamics of the servohydraulic system shown in Fig. 2 can be represented by state space equations to facilitate modern control theory design

$$\dot{\mathbf{z}} = \mathbf{A}\mathbf{z} + \mathbf{B}u \tag{4}$$

$$y = \mathbf{C}\mathbf{z} \tag{5}$$

where $\mathbf{z}$ = state vector; $\dot{\mathbf{z}}$ = time derivative of the state vector; u = system input; y = measured system output; and $\mathbf{A}$, $\mathbf{B}$, and $\mathbf{C}$ = system, input, and output matrices, respectively. The tracking error between the desired and measured displacement is defined by

$$e = r - y \tag{6}$$

The command u to the actuator should be chosen such that the tracking error is minimized. If perfect tracking is achieved, an ideal

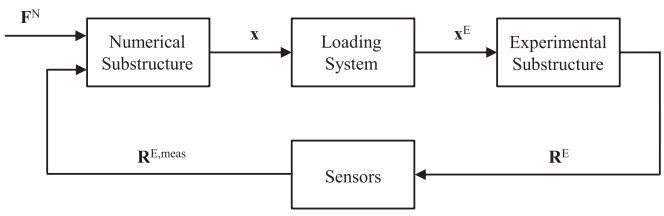

Fig. 1. Schematic of a typical hybrid simulation

J. Struct. Eng., 2013, 139(7): 1205-1214

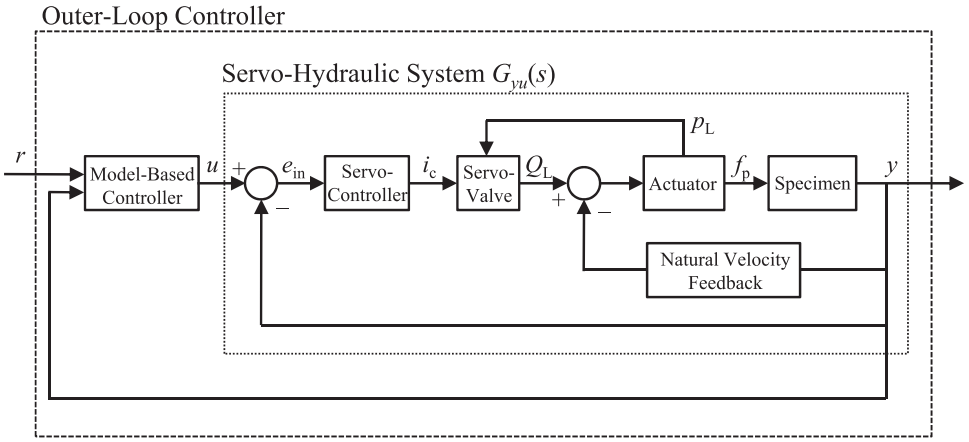

Fig. 2. Block diagram of the outer-loop controller

state $\overline{\mathbf{z}}$ and an ideal input $\overline{u}$ leading to an output $\overline{y}$ must exist such that $\overline{y} = r$. The ideal system is described as

$$\dot{\overline{\mathbf{z}}} = \mathbf{A}\overline{\mathbf{z}} + \mathbf{B}\overline{u} \tag{7}$$

$$\overline{y} = \mathbf{C}\overline{\mathbf{z}} = r \tag{8}$$

Deviations of the state, control, and output from this ideal system with respect to the original system are defined as

$$\tilde{\mathbf{z}} = \mathbf{z} - \overline{\mathbf{z}} \tag{9}$$

$$\tilde{u} = u - \overline{u} \tag{10}$$

$$\tilde{y} = y - \overline{y} \tag{11}$$

The dynamics of the deviation system are then

$$\dot{\tilde{\mathbf{z}}} = \mathbf{A}\tilde{\mathbf{z}} + \mathbf{B}\tilde{u} \tag{12}$$

$$\tilde{y} = \mathbf{C}\tilde{\mathbf{z}} = -e \tag{13}$$

The tracking problem has now been redefined as a regulator problem about a setpoint (Lewis and Syrmos 1995). The control law in Eq. (10) can be rewritten in terms of the original system, which consists of a feedforward component $\overline{u} = u_{FF}$ from the ideal system and a feedback component $\tilde{u} = u_{FB}$ from the deviation system; i.e.,

$$u = \overline{u} + \tilde{u} = u_{FF} + u_{FB} \tag{14}$$

The subsequent section describes how the feedforward and feedback controllers are designed.

Design of Model-Based Servohydraulic Tracking Control

The model-based servohydraulic tracking controller, incorporating feedforward and feedback controllers, is represented schematically in Fig. 3. In contrast to Fig. 2, Fig. 3 shows the detail of the model-based controller block while condensing the servohydraulic system dynamics. The desired displacement r is modified by the feedforward controller and feedback controller to produce the commands u_{FF} and u_{FB}, respectively.

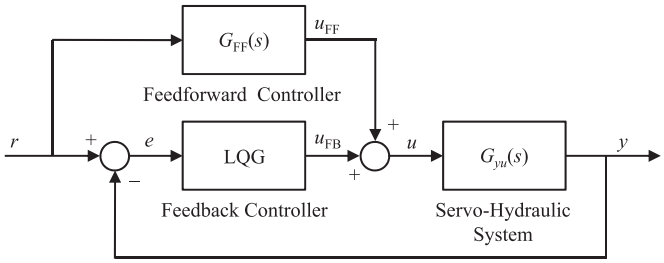

Fig. 3. Block diagram of the feedforward and feedback links

Model-Based Feedforward Controller

To realize the feedforward controller, first a transfer function model of the servohydraulic system is identified from experimental data. The transfer function for the servohydraulic system can typically be represented as

$$G_{yu}(s) = \frac{Y(s)}{U(s)} = \frac{K}{\prod_{i=1}^{N}(s - p_i)} \tag{15}$$

where N = number of poles p_i and K = gain of the model (Carrion and Spencer 2007). Because of the phenomena of the control-structure interaction, this transfer function will be dependent on the physical specimen to which the actuator is attached (Dyke et al. 1995).

The goal of the feedforward controller is to cancel the dynamics of the servohydraulic system using a model inverse. A pure inverse of Eq. (15) would result in an improper transfer function as follows:

$$G_{FF}(s) = \frac{U(s)}{R(s)} = \frac{\prod_{i=1}^{N}(s - p_i)}{K} \tag{16}$$

The proposed approach to implement this improper model inverse is to make use of the displacement, velocity, acceleration, and higher-order derivatives at the interface of the numerical and experimental substructures. Because the specimen should track this trajectory, the velocity, acceleration, and higher-order derivatives can be used as long as the signals are generated quickly and are not contaminated

J. Struct. Eng., 2013, 139(7): 1205-1214

by noise. To avoid introducing additional noise from differentiation, the derivatives should be taken directly from the numerical integration if possible.

The following example demonstrates how to apply this approach to a three-pole transfer function model combined with the central difference method for numerical integration. A three-pole model in Eq. (15) would result in an inverse that is improper by three degrees. In such a case, Eq. (16) can be written as

$$G_{\mathrm{FF}}(s) = \frac{U(s)}{R(s)} = a_0 + a_1 s + a_2 s^2 + a_3 s^3 \tag{17}$$

where coefficients a_0, a_1, a_2, and a_3 are determined by expanding the expression in Eq. (16) for $N = 3$. In the time domain, Eq. (17) becomes

$$u_{\mathrm{FF}}(t) = a_0 r(t) + a_1 \dot{r}(t) + a_2 \ddot{r}(t) + a_3 \dddot{r}(t) \tag{18}$$

where the over dots = differentiation with respect to time. In general, the equations of motion are solved at time step $i - 1$ for the displacements at time step i (i.e., time-stepping numerical integration) and the displacements are imposed on the physical specimen. In discrete time, Eq. (18) can be written as

$$u_{\mathrm{FF},i} = a_0 r_i + a_1 \dot{r}_i + a_2 \ddot{r}_i + a_3 \dddot{r}_i \tag{19}$$

The central difference method is explicit in displacement, thus only the desired displacement r_i is known, where $r_i = x_i$ at the degree of freedom where the actuator is attached. The desired acceleration can be linearly extrapolated over one time step as follows:

$$\ddot{r}_i = \ddot{x}_i = 2\ddot{x}_{i-1} - \ddot{x}_{i-2} \tag{20}$$

The accelerations (and all other signals) must be in relative coordinates such that they describe the desired trajectory of the physical specimen at the actuator interface. The desired velocity can be computed using Eq. (21), which can be derived from the central difference method equations [Eqs. (2) and (3)] as follows:

$$\dot{r}_i = \dot{x}_i = \dot{x}_{i-1} + \frac{\Delta t}{2}(\ddot{x}_{i-1} + \ddot{x}_i) \tag{21}$$

Finally, the desired jerk (derivative of the acceleration) can be calculated directly from the acceleration. Because a linear extrapolation of the acceleration is chosen, the jerk can be calculated as the slope of the extrapolation as follows:

$$\dddot{r}_i = \dddot{x}_i = \frac{1}{\Delta t}(\ddot{x}_{i-1} - \ddot{x}_{i-2}) \tag{22}$$

Depending on the numerical integration scheme and the degree to which the model inverse is improper, the previous procedure may differ. Indeed, there are many other alternatives to estimate higher-order derivatives. Eqs. (20)–(22) were found to produce the most accurate and stable results among the alternatives investigated, which included higher-order and least-squares extrapolations on acceleration as well as extrapolations on all signals. If higher-order derivatives are not available or cannot be calculated accurately, a low-pass filter could be added to Eq. (16) to reduce the degree to which the inverse is improper. With enough poles, the low-pass filter could even create a proper system, as in Carrion and Spencer (2007). However, low-pass filters typically introduce unwanted dynamics into the feedforward controller. In some applications, the displacement signal is known a priori (e.g., earthquake motion reproduction); for such cases, smooth derivatives can be created offline.

Model-Based Feedback Controller

In the presence of changing specimen conditions, modeling errors, and disturbances, LQG control can be applied to the deviation system to bring the deviation states to zero and thus reduce the tracking error. The deviation system is rewritten as

$$\dot{\tilde{\mathbf{z}}} = \mathbf{A}\tilde{\mathbf{z}} + \mathbf{B}u_{\mathrm{FB}} + \mathbf{E}w_{\mathrm{f}} \tag{23}$$

$$\tilde{y} = \mathbf{C}\tilde{\mathbf{z}} + v_{\mathrm{f}} \tag{24}$$

where w_{f} = disturbance to the system and v_{f} = measurement noise. Because the states of the servohydraulic system model do not correspond to measureable quantities, only the output of the deviation system (i.e., $\tilde{y} = y - r$) is measurable. Thus, an observer is needed to estimate the unknown states of the deviation system. Evoking the separation principal, a LQG controller can be designed from independent LQR (optimal state feedback control) and Kalman filter (optimal observer) designs (Stengel 1986).

To improve the LQG controller's tracking performance and robustness in the frequency range of interest, the disturbance w_{f} is assumed to be Gaussian white noise w passed through a second-order shaping filter; i.e.

$$\dot{\mathbf{z}}_{\mathrm{f}} = \mathbf{A}_{\mathrm{f}}\mathbf{z}_{\mathrm{f}} + \mathbf{E}_{\mathrm{f}}w \tag{25}$$

$$w_{\mathrm{f}} = \mathbf{C}_{\mathrm{f}}\mathbf{z}_{\mathrm{f}} \tag{26}$$

where

$$\mathbf{A}_{\mathrm{f}} = \begin{bmatrix} 0 & 1 \\ -\omega_{\mathrm{f}}^2 & -2\xi_{\mathrm{f}}\omega_{\mathrm{f}} \end{bmatrix}, \quad \mathbf{E}_{\mathrm{f}} = \begin{bmatrix} 0 \\ 1 \end{bmatrix}, \quad \text{and} \quad \mathbf{C}_{\mathrm{f}} = \begin{bmatrix} \omega_{\mathrm{f}}^2 & 2\xi_{\mathrm{f}}\omega_{\mathrm{f}}\eta_{\mathrm{f}} \end{bmatrix} \tag{27}$$

The parameters ξ_{f}, ω_{f}, and η_{f} control the peak, bandwidth, and roll-off of the disturbance, respectively. The deviation system of Eqs. (23) and (24) can be rewritten as an augmented system that includes the dynamics of the shaping filter. The LQR controller and Kalman filter should then be designed based on the augmented system.

Experimental Setup and Characterization

To demonstrate the efficacy of the proposed model-based servohydraulic tracking controller, a 9-story model building with MR dampers installed was investigated. Semiactive control devices such as MR dampers combine the desirable properties of both passive and active control devices. They have the ability to adapt to loading demands on the structure, as in an active control system; however, as with passive systems, they cannot inject energy into the system, eliminating stability concerns. With a MR damper, changes in the input current can be used to achieve forces predictably in advanced semiactive control algorithms (Spencer et al. 1997). By using RTHS as the experimental framework, the building can be modeled numerically while the MR dampers can be tested experimentally.

The RTHS testing system at the University of Illinois is located in the Newmark Structural Engineering Laboratory (http://nsel.cee.illinois.edu) and is a part of the Smart Structures Technology Laboratory (http://sstl.cee.illinois.edu). The actuator is rated at 556 kN (125 kip) with a stroke of ± 152.4 mm (± 6 in.) and effective piston area of 271 cm^2 (42 $in.^2$). The displacement of the actuator is measured using an internal alternating current LVDT. A 445 kN

J. Struct. Eng., 2013, 139(7): 1205-1214

(100 kip) Key Transducers, Inc., load cell in line with the actuator measures the restoring force of the attached specimen. This setup (see Fig. 4) has proven successful for the dynamic testing of large-scale MR dampers (Yang et al. 2002; Phillips et al. 2010). A dSPACE Model 1103 digital signal processing board is used to perform numerical integration of the equations of motion for the numerical substructure, apply the real-time servohydraulic control, and implement semiactive control algorithms.

Magnetorheological Damper Specimen

The test specimen used in this paper is a second-generation, large-scale 200-kN MR damper manufactured by the Lord Corporation. The damper has a stroke of ± 292 mm (±13 in.) and can generate forces slightly higher than the nominal 200 kN. The damper has an accumulator charged to 5.17 MPa (750 psi) to compensate for the thermal expansion of the MR fluid (Christenson et al. 2008).

The current to the MR damper is controlled using a pulse-width modulator (PWM), which consists of an unregulated power supply providing 80 V [direct current (DC)] to an Advanced Motion Controls Model 20a8 analog servodrive. The MR damper responds to increases in applied current with corresponding increases in the restoring force during dynamic events. The responses of the damper to a 25.4 mm, 1 Hz sine wave at six different levels of input current are presented in Fig. 5. As can be seen, the response is velocity dependent and highly nonlinear. At the same time, the magnitude of the restoring force changes dramatically, yet predictably, with the input current. This characteristic makes MR dampers ideal for semiactive structural control.

Identification of the Servohydraulic System Model

The transfer function from the input commanded displacement to the output measured displacement $G_{yu}(s)$ of the servohydraulic system was calculated over a wide range of frequencies. This transfer function includes the dynamics of the actuator, servovalve, servo-controller, and specimen. The input was selected as band-limited white noise (BLWN) from 0 to 50 Hz with a displacement RMS of 0.254 mm, providing insight into the servohydraulic dynamics over this range of frequencies.

Because the current to the MR damper can change during the RTHS, the servohydraulic dynamics must be investigated at multiple current levels. The measured transfer function magnitude, phase, and time lag are presented in Fig. 6 for two conditions; i.e., 0.0 and 2.5 A. The results are also averaged to create a third transfer function at average conditions. Time lag is calculated by dividing the phase by the frequency, which is sensitive to noise at the lower frequencies.

The identified transfer function models are overlain in Fig. 6 in dashed black lines. The three-pole models were found sufficient to accurately represent the dynamics over the frequency range of interest (up to 40 Hz). The models of the servohydraulic dynamics at 0.0 and 2.5 A, as well as the average of the two specimen conditions, are given by

$$G_{yu,0.0\mathrm{A}}(s) = \frac{1.730 \times 10^7}{(s + 182.7)(s^2 + 225.3s + 9.499 \times 10^4)} \tag{28}$$

$$G_{yu,2.5\mathrm{A}}(s) = \frac{1.613 \times 10^7}{(s + 134.2)(s^2 + 324.6s + 1.211 \times 10^5)} \tag{29}$$

$$G_{yu,\mathrm{avgA}}(s) = \frac{1.600 \times 10^7}{(s + 151.7)(s^2 + 250.4s + 1.061 \times 10^5)} \tag{30}$$

Fig. 6 shows that the behavior of the servohydraulic system is also frequency dependent, where the magnitude and phase (or, equivalently, the time lag) vary with frequency. Traditional delay compensation approaches based on a single constant time delay would be inadequate for systems that respond at multiple frequencies, such as MDOF structures. Likewise, traditional approaches do not address the decay in magnitude observed.

The typical time delays/lags reported in the literature range from 8 to 30 ms (Horiuchi et al. 1999; Nakashima and Masaoka 1999; Darby et al. 2002; Carrion and Spencer 2007; Wallace et al. 2007; Chen and Ricles 2010). The time lag in this experimental setup was found to vary between 8 and 11 ms depending on the frequency of excitation and the specimen conditions, which is relatively small for such a large actuator. Subsequent tests comparing the lag between input sine waves and measured responses confirmed these results.

Experimental Evaluation of the Feedforward-Feedback Design

Real-time servohydraulic controllers were created based on the model-based methods proposed, previous model-based approaches with a low-pass filter (Carrion and Spencer 2007), the third-order polynomial extrapolation method (Horiuchi et al. 1996), and lead compensator approaches. The model-based controllers were designed using the identified models in Eqs. (28)–(30), while the polynomial extrapolation and lead compensator controllers were designed to compensate for the DC (i.e., low-frequency) time lag observed in Fig. 6. Table 1 summarizes the controllers explored, identified by the controller type and specimen condition.

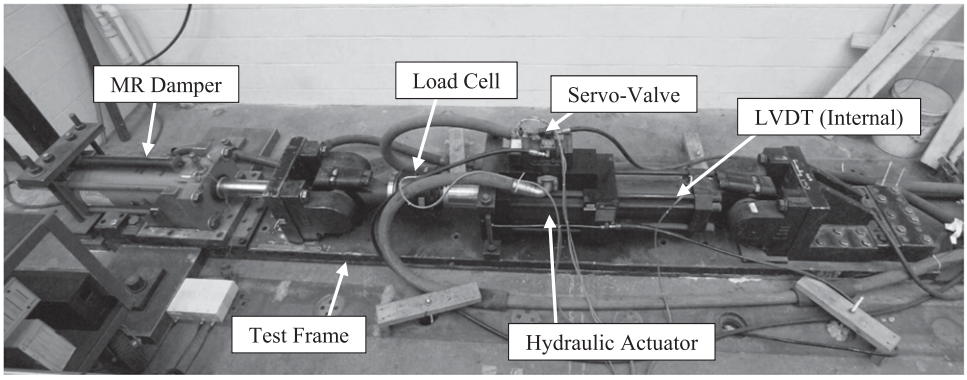

Fig. 4. Test frame at the University of Illinois

J. Struct. Eng., 2013, 139(7): 1205-1214

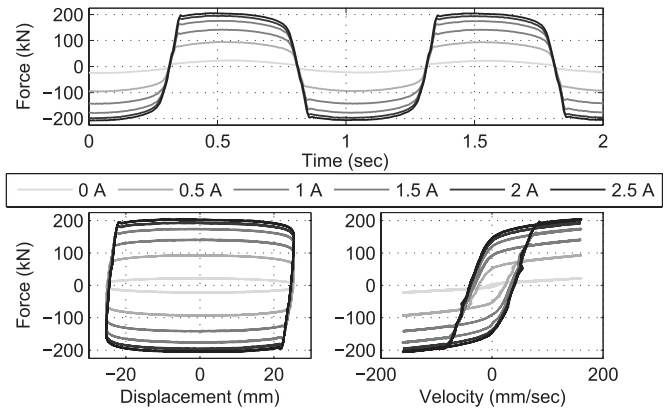

Fig. 5. MR damper response to a 25.4 mm, 1 Hz sine wave at select levels of current

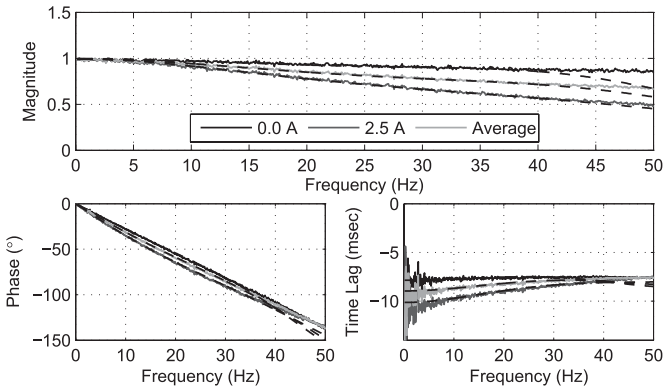

Fig. 6. Measured system transfer functions $G_{yu}(s)$ at select current levels (dashed lines represent fitted transfer function models)

Table 1. Real-Time Servohydraulic Controller Types

Specimen condition	Short name
Proposed model-based tracking control	
0.0 A	$G_{\mathrm{FF},0.0\mathrm{A}}(s)$
2.5 A	$G_{\mathrm{FF},2.5\mathrm{A}}(s)$
Average/general	$G_{\mathrm{FF,avgA}}(s)$ + LQG
Model-based control with low-pass filter	
0.0 A	$G_{\mathrm{FF},0.0\mathrm{A}}(s)$ + LP
2.5 A	$G_{\mathrm{FF},2.5\mathrm{A}}(s)$ + LP
Average/general	Bumpless + LP
Third-order polynomial extrapolation	
0.0 A	3rd Poly 8ms
2.5 A	3rd Poly 10ms
Average/general	3rd Poly 9ms
Lead compensator (single pole, single zero)	
0.0 A	Lead Comp 8ms
2.5 A	Lead Comp 10ms
Average/general	Lead Comp 9ms

Tracking Performance in the Frequency Domain

To evaluate the performance in the frequency domain, the real-time servohydraulic controllers were implemented in *dSPACE*. Then, BLWN from 0 to 50 Hz with a displacement RMS of 0.254 mm was commanded to experimentally determine the compensated servohydraulic system transfer function $G_{yr}(s)$ (see Fig. 3). The controllers were designed to match the specimen conditions, with results for the 0.0-A condition in Fig. 7 and the 2.5-A condition in Fig. 8. Perfect controller performance would be indicated by the unity magnitude, zero phase, and zero time lag over the frequency range of interest.

The polynomial extrapolation technique provided good compensation at low frequencies. However, magnitude undershoot was found from 5 to 15 Hz, whereas above 15 Hz the magnitude began to increase dramatically. Because of this amplification, the system was not excited above 30 Hz for safety. At the same time, the polynomial extrapolation technique overcompensated for the time lag after 10 Hz. This overcompensation can add positive damping to the RTHS loop, adding stability while compromising accuracy. After about 25 Hz, the polynomial extrapolation technique begins to undercompensate.

The lead compensator also provided good compensation at low-frequencies. However, at about 10 Hz, the magnitude began to increase significantly and the time lag became undercompensated. A single pole and zero pair were not enough to provide adequate

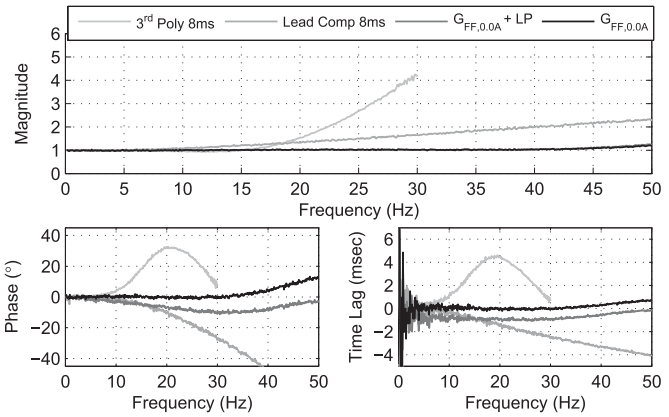

Fig. 7. Transfer functions $G_{yr}(s)$ for various control techniques with 0.0 A in the damper

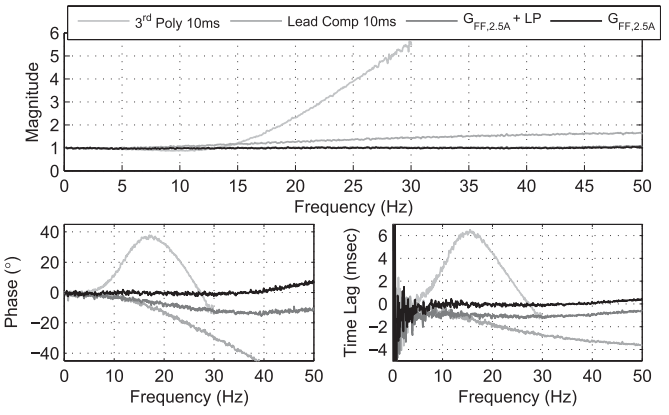

Fig. 8. Transfer functions $G_{yr}(s)$ for various control techniques with 2.5 A in the damper

J. Struct. Eng., 2013, 139(7): 1205-1214

compensation over a broad frequency range, which can be problematic if high-frequency response is expected.

These results demonstrate that the model-based approaches have significantly better performance in terms of both magnitude and phase (or time lag). Excellent results can be seen in magnitude performance for model-based approaches up to 50 Hz. In terms of phase, the model-based approach using a low-pass filter has slightly poorer time lag compensation, which is a result of the dynamics of the low-pass filter adversely adding approximately 1-ms phase lag at all frequencies to the model-based inverse.

Tracking Performance in the Time Domain

Real-time servohydraulic control was also evaluated in the time domain using a predefined displacement and current command history. Two displacement histories were explored; i.e., (1) BLWN with a bandwidth of 0–5 Hz and a RMS of 2.78 mm, and (2) BLWN with a bandwidth of 0–15 Hz and a RMS of 0.595 mm. The merits of these tests are that by restricting the bandwidth, much higher velocities are possible, for which control can be challenging.

During these tests, the current command to the MR damper was either maintained at 0.0 or 2.5 A, or at a pulse between 0.0 and 2.5 A at 0.5 Hz (50% duty cycle, mimicking semiactive control conditions). The results of the time domain tracking tests are presented in Table 2. Good tracking is indicated by a low RMS error (norm) between the desired and measured displacements as calculated by

$$\text{RMS error (norm)} = \sqrt{\frac{\sum_i^N (r_i - y_i)^2}{\sum_i^N (r_i)^2}} \times 100\% \qquad (31)$$

where r_i = desired displacement and y_i = measured displacement at the ith time step.

Table 2. Tracking Performance for Predefined Displacement Histories

Controller	RMS % error (0–5 Hz BLWN)	RMS % error (0–15 Hz BLWN)
Specimen condition: 0.0 A		
None	16.0	42.9
3rd Poly 8ms	1.22	12.8
Lead Comp 8ms	1.95	13.3
$G_{FF,0.0A}(s)$ + LP	1.01	4.27
$G_{FF,0.0A}(s)$	0.942	3.45
$G_{FF,avgA}(s)$ + LQG	1.16	3.89
Specimen condition: 2.5 A		
None	20.1	51.7
3rd Poly 10ms	2.04	25.9
Lead Comp 10ms	3.34	15.1
$G_{FF,2.5A}(s)$ + LP	2.55	9.40
$G_{FF,2.5A}(s)$	2.27	4.68
$G_{FF,avgA}(s)$ + LQG	1.41	5.57
Specimen condition: 2.5 A pulse		
None	18.1	49.2
3rd Poly 9ms	1.80	18.3
Lead Comp 9ms	2.97	16.0
Bumpless + LP	2.04	8.45
$G_{FF,avgA}(s)$	1.93	6.35
$G_{FF,avgA}$ + LQG	1.09	4.72

Note: BLWN = band-limited white noise.

The results highlight that the proposed model-based servohydraulic tracking control technique provides considerable improvement in system performance through reduction of the RMS error for all specimen conditions. The model-based feedforward controllers designed to match the specimen conditions performed well while the general model-based feedforward-feedback controller performed well under all specimen conditions.

Real-Time Hybrid Simulation Study of the Single-Degree-of-Freedom System

To illustrate the real-time servohydraulic controller performances in a closed-loop RTHS, a simple SDOF structure was selected. Mass, damping, and stiffness were simulated numerically while a MR damper at 0.0 A was used as the physical substructure. At this level of current, the MR damper can create an approximately 20-kN restoring force, which would provide an appropriate level of control (approximately 10% of the mass) for a 20,000-kg structure. With the mass held constant, the stiffness was varied to achieve a set of structures with natural frequencies ranging from 0.5 to 30 Hz. Although it is not likely that a civil engineering structure will have a single natural frequency so high, MDOF structures may possess natural frequencies in this range or beyond. For each structure, the damping coefficient was chosen to achieve 2% damping.

Each structure was excited with BLWN ground acceleration from 0 to 30 Hz. The RMS values of the ground acceleration were chosen as 1,000 mm/s^2 for the 0.5 and 1 Hz structures, 1,500 mm/s^2 for the 5 Hz structure, and 2,000 mm/s^2 for the 10, 20, and 30 Hz structures. These RMS values were chosen to provide a safe level of excitation while achieving a response significantly above the noise floor of the measurement devices. Each structure was tested using no compensation, the third-order polynomial extrapolation, a lead compensator, model-based feedforward control with a low-pass filter, and the proposed model-based feedforward control with and without feedback. The results are presented in Fig. 9 with each experiment summarized by the RMS error between the desired and measured displacement.

All real-time servohydraulic control schemes provided improved tracking when compared with the uncompensated case, except for the third-order polynomial extrapolation for the 30-Hz structure. In this case, the response became so greatly amplified that the experiment was unsafe to continue. The third-order polynomial extrapolation and lead compensators were not accurate in magnitude or phase at higher frequencies, leading to poor performance in RTHS. The model-based feedforward controller with a low-pass filter worked well; however, the added low-pass filter dynamics detracted from controller performance, especially at higher frequencies. The proposed model-based feedfoward controller exhibited the best results over a wide range of frequencies. Thus, if a structure exhibits higher-frequency responses, the proposed method would be able to provide the best tracking and avoid instability. Adding model-based feedback control further improves performance over the lower-frequency region (as was desired for this particular feedback controller design).

High-Fidelity Magnetorheological Damper Model

To assist in developing semiactive control algorithms and verify experimental results, a high-fidelity MR damper model was created based on the phenomenological model proposed by Spencer et al. (1997). Fig. 10 illustrates the underlying mechanics of the model, which relate an input displacement x to an output restoring force F. Equating the forces on either side of the center rigid bar in Fig. 10 leads to the following relationship:

J. Struct. Eng., 2013, 139(7): 1205-1214

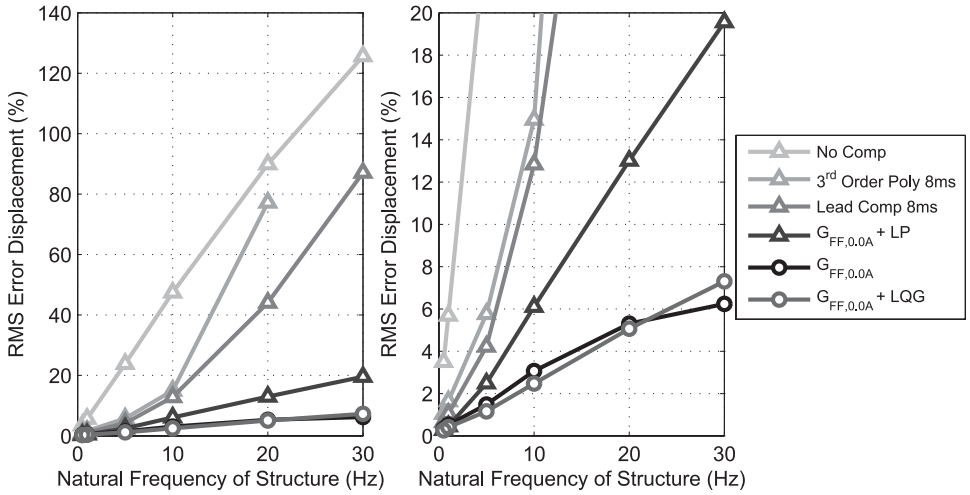

Fig. 9. RMS error for RTHS of a SDOF structure

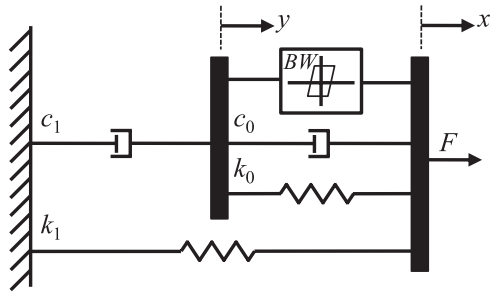

Fig. 10. Phenomenological model of a MR damper

$$c_1\dot{y} = \alpha z + k_0(x-y) + c_0(\dot{x}-\dot{y}) \tag{32}$$

The force αz is determined by the evolutionary variable z modeled by a Bouc-Wen hysteretic element (Baber and Wen 1981)

$$\dot{z} = -\gamma|\dot{x}-\dot{y}||z|z|^{n-1} - \beta(\dot{x}-\dot{y})|z|^n + A(\dot{x}-\dot{y}) \tag{33}$$

The restoring force F can be described by equating the forces on either side of the right-hand-side rigid bar in Fig. 10 as

$$F = \alpha z + c_0(\dot{x}-\dot{y}) + k_0(x-y) + k_1(x-x_0) \tag{34}$$

Because the MR damper piston rod is double ended, no force offset is present under zero displacement; thus, the stiffness term k_1 can be set to zero. The other model parameters were fit using Simulink's parameter estimation tool within *MATLAB*. To model the current-dependent behavior of the MR damper, Eqs. (35)–(39) were incorporated into the model, where i_c is the input current. Parameters with the subscript a were fit to the 0.0-A data, while parameters with subscript b were fit to the 2.5-A data. An exponential relationship between the extremes was found best to match the behavior intermediate levels of current, with the rate of change described by the parameters with subscript c. The optimized parameters are presented in Table 3

$$\alpha = \alpha_b + (\alpha_a - \alpha_b) \times \exp(-\alpha_c i_c) \tag{35}$$

$$c_0 = c_{0,b} + (c_{0,a} - c_{0,b}) \times \exp(-c_{0,c} i_c) \tag{36}$$

$$c_1 = c_{1,b} + (c_{1,a} - c_{1,b}) \times \exp(-c_{1,c} i_c) \tag{37}$$

$$\beta = \beta_b + (\beta_a - \beta_b) \times \exp(-\beta_c i_c) \tag{38}$$

$$\gamma = \gamma_b + (\gamma_a - \gamma_b) \times \exp(-\gamma_c i_c) \tag{39}$$

In addition to the current-dependent behavior of the MR damper at static levels of current, changes in current introduce dynamics that must be modeled. These dynamics can be described as a time lag consisting of the following two components: (1) the lag between when a current is commanded to the PWM device and when it is realized in the MR damper circuit, and (2) the lag between when the current is realized in the MR damper circuit and when the corresponding restoring force is achieved in the MR damper. The aggregate effects of both lags are modeled by a first-order transfer function [Eq. (40)] curve fit to match experimental data. The desired current i_d is input to the transfer function and the effective resulting current i_c is then input to the MR damper model. A second-order low-pass filter with a cutoff frequency of 75 Hz is added in series with Eq. (40) to avoid model stability issues sometimes found for quickly changing current in numerical simulation

$$i_c = \frac{(s+9\pi)}{9(s+\pi)} i_d \tag{40}$$

Real-Time Hybrid Simulation of a Multiple-Degree-of-Freedom Semiactively Controlled Structure

To verify the model-based servohydraulic tracking control technique for large-scale real-time hybrid simulation, a well-researched 9-story steel shear frame benchmark building was chosen (Ohtori et al. 2004). This structure was designed to meet the seismic code and represent a typical medium-rise building in Los Angeles, California. The north-south (NS) lateral load system consisted of two identical moment-resisting frames. For this research, a linear model of one of

these NS moment-resisting frames was used with half of the total seismic mass of the structure and was excited in the NS direction.

The natural frequencies of the structure corresponding to the first five modes were 0.443, 1.18, 2.05, 3.09, and 4.27 Hz, respectively, with a maximum natural frequency of 63.6 Hz at the twenty-ninth mode. All modes were assumed to have 2% damping. Because the central difference method was chosen, no numerical damping was added from the integration scheme.

The structural control provided by MR dampers (added to the structure for this study) was assumed to keep the response of the structure in the linear range for the earthquakes investigated. To achieve a reasonable level of control, eighteen 200-kN MR dampers were added between the ground and the first story. By doing so, the need to test multiple devices was eliminated because the force from one MR damper can represent all 18 (the floors were assumed to be rigid bodies). MR dampers with higher capacities have been developed; thus, it is possible to reduce the number of dampers in a practical implementation. In this study, the MR dampers were represented by a physical specimen, while the rest of the structure was simulated numerically.

Table 3. Phenomenological Model Parameters for the 200-kN MR Damper

Parameter	Value
$c_{0,a}$	0.080 kN·s/mm
$c_{0,b}$	0.32 kN·s/mm
$c_{0,c}$	1.5 A^{-1}
k_0	0.0 kN/mm
k_1	0.0 kN/mm
x_0	0.0 mm
$c_{1,a}$	3.0 kN·s/mm
$c_{1,b}$	15.0 kN·s/mm
$c_{1,c}$	2.0 A^{-1}
α_a	0.11 kN/mm
α_b	0.55 kN/mm
α_c	1.0 A^{-1}
γ_a, β_a	0.050 mm^{-2}
γ_b, β_b	0.0020 mm^{-2}
γ_c, β_c	5.2 A^{-1}
A	300
n	2.0

The semiactive controller used was based on the clipped-optimal control algorithm (Dyke et al. 1996). The semiactive controller was designed with equal weighting on all story absolute accelerations paired with low weighting of the MR damper force. These weightings achieve good semiactive control results in simulation over a wide range of earthquake records. More details applying semiactive control to large-scale MR dampers, including compensation techniques for the damper response lag, can be found in Friedman et al. (2010) and Phillips et al. (2010).

RTHS was used to evaluate the response of the 9-story structure subjected to the NS component of the 1940 El Centro earthquake with a scale factor of 0.5 (peak ground acceleration of 0.174g). Numerical integration was performed using the central difference method with a sampling rate of 2,000 Hz. The results are presented in Fig. 11 with time histories of the displacement and force of the MR damper specimen shown along with the force-displacement hysteresis and the force-velocity hysteresis. The numerical simulation results are also presented using the proposed phenomenological model to represent the MR damper specimen.

The RTHS quickly became unstable in the absence of compensation; therefore, uncompensated results are not presented. The semiactive control switched the specimen conditions between the extremes very quickly, adding high-frequency dynamics to the structure. The third-order polynomial extrapolation technique significantly amplified these dynamics, leading toward high-amplitude oscillations in the force, which was most apparent in the hysteresis. On the other hand, the results were similar for both the model-based controller with bumpless transfer scheduling control (Carrion and Spencer 2007) and the proposed model-based feedforward-feedback tracking controller. Small oscillations in the force were apparent with the bumpless transfer controller, which were caused by the low-pass filter adding phase lag to the controller. The additional lag (as seen in Figs. 7 and 8) led to negative damping and small oscillations; the oscillations did not grow appreciably because as the MR damper moved positive damping was added to the system.

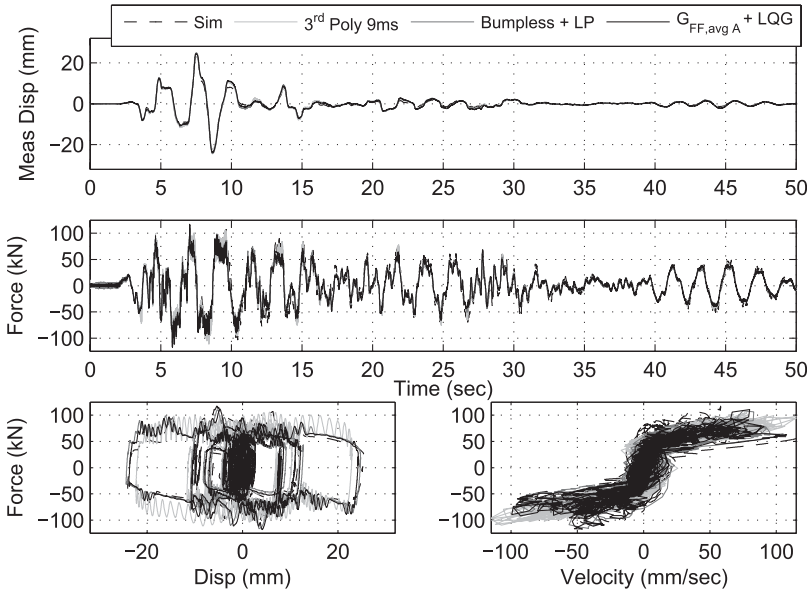

Fig. 11. MR damper response using semiactive control

J. Struct. Eng., 2013, 139(7): 1205-1214

The proposed model-based servohydraulic tracking control strategy for this application (three-pole transfer function models with the central difference method) required an extrapolation of the acceleration followed by a prediction of velocity. The RMS error between the extrapolated acceleration and the actual acceleration one time step later was 1.81%. The RMS error between the predicted velocity and actual velocity one time step later was 0.0061%. The low RMS error indicates that the extrapolated and predicted values provide accurate estimates toward implementing an improper inverse.

The numerical simulation matched the RTHS well, providing confidence in the results. The differences can be attributed to the difficulty in modeling the behavior of the MR damper under changing current, as well as the semiactive control affecting future control efforts. These challenges aside, the model provides a good comparison even for the semiactive case and, more importantly, a useful tool for semiactive controller design. Further results, including RTHS for passive-off and passive-on cases of the 9-story structure, can be found in Phillips and Spencer (2011).

Conclusions

This paper provides a framework for model-based servohydraulic tracking control including both model-based feedforward and feedback links to directly address added, unwanted dynamics in the RTHS loop. A simple approach to developing a model-based servohydraulic tracking controller for a general servohydraulic system has been proposed. With predefined displacements, the results showed near-perfect tracking of the desired displacement signal. In RTHS, the proposed model-based controller was proven successful for testing SDOF structures in a parametric study and a lightly damped MDOF structure, both using a 200-kN MR damper as the physical substructure. In the SDOF test, the proposed model-based controller provided the best tracking among the methods considered, especially when the natural frequency of the structure exceeded 5 Hz. In the MDOF test, the current in the MR damper was allowed to vary under semiactive control. Even under these changing specimen conditions, which introduce higher-frequency dynamics into the RTHS, the proposed model-based controller showed excellent performance. For the numerical simulations, a phenomenological model is proposed to accurately represent the 200-kN MR damper dynamics under semiactive conditions. The numerical simulation results compared well with RTHS, proving confidence in the RTHS results.

Acknowledgments

The authors acknowledge the support of the National Science Foundation under Award No. CMMI-1011534, as well as Richard E. Christenson for the use of the 200-kN MR damper.

References

Baber, T. T., and Wen, Y. K. (1981). "Random vibration hysteretic, degrading systems." *J. Engrg. Mech. Div.*, 107(6), 1069–1087.

Carrion, J. E. and Spencer Jr., B. F. (2007). "Model-based strategies for real-time hybrid testing." *Newmark Structural Engineering Laboratory Rep. No. 6*, Univ. of Illinois at Urbana-Champaign, Urbana, IL.

Carrion, J. E., Spencer, B. F., Jr., and Phillips, B. M. (2009). "Real-time hybrid simulation for structural control performance assessment." *Earthquake Eng. Eng. Vib.*, 8(4), 481–492.

Chen, C., and Ricles, J. M. (2010). "Tracking error-based servohydraulic actuator adaptive compensation for real-time hybrid simulation." *J. Struct. Eng.*, 136(4), 432–440.

Christenson, R. E., Lin, Y., Emmons, A., and Bass, B. (2008). "Large-scale experimental verification of semi-active control through real-time hybrid simulation." *J. Struct. Eng.*, 134(4), 522–534.

Darby, A. P., Blakeborough, A., and Williams, M. S. (1999). "Real-time substructure tests using hydraulic actuator." *J. Eng. Mech.*, 125(10), 1133–1139.

Darby, A. P., Williams, M. S., and Blakeborough, A. (2002). "Stability and delay compensation for real-time substructure testing." *J. Eng. Mech.*, 128(12), 1276–1284.

Dyke, S. J., Spencer, B. F., Jr., Quast, P., and Sain, M. K. (1995). "Role of control-structure interaction in protective system design." *J. Eng. Mech.*, 121(2), 322–338.

Dyke, S. J., Spencer, B. F., Jr., Sain, M. K., and Carlson, J. D. (1996). "Modeling and control of magnetorheological dampers for seismic response reduction." *Smart Mater. Struct.*, 5(5), 565–575.

Friedman, A. J., et al. (2010). "Accommodating MR damper dynamics for control of large scale structural systems." *Proc., 5th World Conf. on Structural Control and Monitoring*, Japan Society for the Promotion of Science (JSPS), Tokyo.

Horiuchi, T., Inoue, M., Konno, T., and Namita, Y. (1999). "Real-time hybrid experimental system with actuator delay compensation and its application to a piping system with energy absorber." *Earthquake Eng. Struct. Dyn.*, 28(10), 1121–1141.

Horiuchi, T., and Konno, T. (2001). "A new method for compensating actuator delay in real-time hybrid experiments." *Philos. Trans. R. Soc. London, Ser. A*, 359(1786), 1893–1909.

Horiuchi, T., Nakagawa, M., Sugano, M., and Konno, T. (1996). "Development of a real-time hybrid experimental system with actuator delay compensation." *Proc., 11th World Conf. on Earthquake Engineering*, International Association for Earthquake Engineering (IAEE), Tokyo.

Jung, R. Y., Shing, P. B., Stauffer, E., and Thoen, B. (2007). "Performance of a real-time pseudodynamic test system considering nonlinear structural response." *Earthquake Eng. Struct. Dyn.*, 36(12), 1785–1809.

Lewis, F. L., and Syrmos, V. L. (1995). *Optimal control*, 2nd Ed., Wiley-Interscience, New York, 377–393.

MATLAB [Computer software]. Natick, MA, MathWorks.

Nakashima, M., Kato, H., and Takaoka, E. (1992). "Development of real-time pseudo dynamic testing." *Earthquake Eng. Struct. Dyn.*, 21(1), 79–92.

Nakashima, M., and Masaoka, N. (1999). "Real time on-line test for MDOF systems." *Earthquake Eng. Struct. Dyn.*, 28(4), 393–420.

Ohtori, Y., Christenson, R. E., Spencer, B. F., Jr., and Dyke, S. J. (2004). "Benchmark control problems for seismically excited nonlinear buildings." *J. Eng. Mech.*, 130(4), 366–385.

Phillips, B. M., et al. (2010). "Real-time hybrid simulation benchmark structure with a large-scale MR damper." *Proc., 5th World Conf. on Structural Control and Monitoring*, Japan Society for the Promotion of Science (JSPS), Tokyo.

Phillips, B. M., and Spencer, B. F., Jr. (2011). "Model-based feedforward-feedback tracking control for real-time hybrid simulation." *Newmark Structural Engineering Laboratory Rep. No. 28*, Univ. of Illinois at Urbana-Champaign, Urbana, IL.

Soong, T. T., and Spencer, B. F., Jr. (2002). "Supplemental energy dissipation: State-of-the-art and state-of-the-practice." *Eng. Struct.*, 24(3), 243–259.

Spencer, B. F., Jr., Dyke, S. J., Sain, M. K., and Carlson, J. D. (1997). "Phenomenological model for magnetorheological dampers." *J. Eng. Mech.*, 123(3), 230–238.

Stengel, R. F. (1986). *Stochastic optimal control: Theory and application*, Wiley, New York.

Wallace, M. I., Wagg, D. J., Neild, S. A., Bunnis, P., Lieven, N. A. J., and Crewe, A. J. (2007). "Testing coupled rotor blade-lag damper vibration using real-time dynamic substructuring." *J. Sound Vib.*, 307(3–5), 737–754.

Wu, B., Bao, H., Ou, J., and Tian, S. (2005). "Stability and accuracy analysis of the central difference method for real-time substructure testing." *Earthquake Eng. Struct. Dyn.*, 34(7), 705–718.

Yang, G., Spencer, B. F., Jr., Carlson, J. D., and Sain, M. K. (2002). "Large-scale MR fluid dampers: modeling and dynamic performance considerations." *Eng. Struct.*, 24(3), 309–323.